ANNALS OF GEOPHYSICS, 59, Fast Track 5, 2016; DOI: 10.4401/ag-7299

Minor shallow gravitational component on the Mt. Vettore surface ruptures related to M_W 6, 2016 Amatrice earthquake

MATTEO ALBANO[1], MICHELE SAROLI[2,1], MARCO MORO[1], EMANUELA FALCUCCI[1], STEFANO GORI[1], SALVATORE STRAMONDO[1], FABRIZIO GALADINI[1], SALVATORE BARBA[1*]

[1]Istituto Nazionale di Geofisica e Vulcanologia, via di Vigna Murata 605, 00143 Roma (Italy)

[2]Dipartimento di Ingegneria Civile e Meccanica (DICeM), Università degli Studi di Cassino e del Lazio meridionale, via G. di Biasio 43, 03043, Cassino (Italy).

matteo.albano@ingv.it

Abstract

On 24th August 2016 a M_W 6.0 earthquake occurred near Amatrice (central Italy) causing nearly 300 fatalities. The mainshock ruptured a NNW-SSE striking, WSW dipping normal fault. The earthquake produced several coseismic effects at ground, including landslides and ground ruptures. In particular, ground surveys identified a 5.2 km long continuous fracture along the Mt. Vettore flank, both on rock and slope deposits, along one of the active normal fault segments bounding the relief to the west. In this work, we evaluated the contribution of seismically-induced surface instabilities to the observed ground fractures by means of a permanent-displacement approach. The results of a parametric analysis show that the computed seismically-induced gravitational displacements (about 2-10 cm) are not enough to explain field observations, testifying to a mean 20-25 cm vertical offset. Thus, the observed ground fractures are the result of primary faulting related to tectonics, combined with gravitational phenomena.

I. INTRODUCTION

On August 24th 2016 a M_W 6.0 normal faulting earthquake occurred near Amatrice (Central Italy), approximately 50 km NW of L'Aquila (Figure 1a). Almost 300 people were killed and three villages were partially destroyed. About 11500 aftershocks occurred in the first month after the mainshock, including 200 with magnitude between 3 and 4, 14 between 4 and 5 and one of M_W 5.4 (Figure 1a) [ISIDe Working Group, 2016].

Preliminary inversion models performed with GPS, SAR and strong-motion data revealed the geometry and the coseismic slip distribution of the mainshock causative fault

* Guest author.

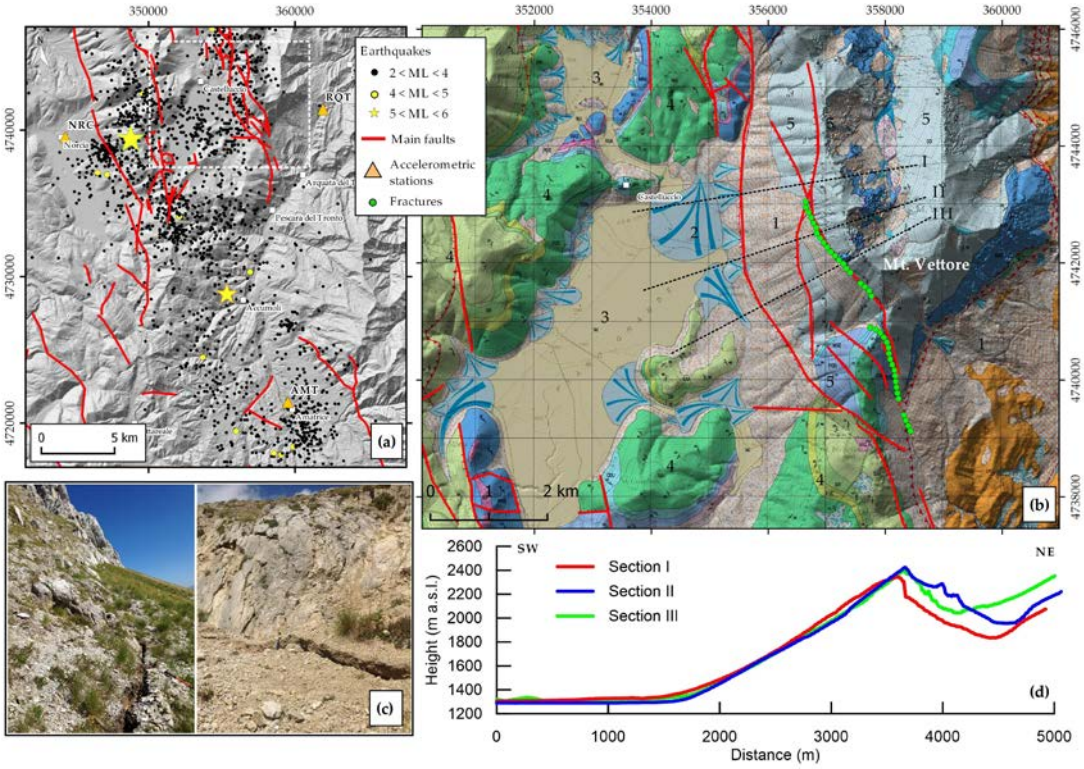

Figure 1: *(a) Location of the mainshock and aftershocks. The Mw 6.0 mainshock and the Mw 5.4 aftershock are represented by yellow stars with red and green stroke, respectively. (b) Detail of Mt. Vettore area (white square in panel a). The numbered lithologies are: 1- Slope deposits; 2- Alluvial deposits; 3- Fluvio-lacustrine deposits; 4- Marly limestones and calcilutites; 5- Limestones and marly limestones (modified from Pierantoni et al. [2013]). (c) Pictures of the observed fractures on Mt. Vettore flank. (d) Topographic profiles along sections I, II and III in panel b.*

[Gruppo di Lavoro INGV sul terremoto di Amatrice, 2016].

The mainshock produced several coseismic effects at ground, including landslides and ground ruptures along mountain slopes and cultivated fields [EMERGEO Working Group, 2016]. In particular, a continuous coseismic rupture, approximately 5.2 km long, was observed on the SW flank of Mt. Vettore, along the Vettore and Vettoretto active normal-faults (Figure 1b and c). This newly formed fracture was observed both on slope deposits and on the bedrock fault planes. Such fractures were initially interpreted as primary surface faulting, although satellite measurements revealed localized displacements in the area, extending for about 0.5 km² on the Mt. Vettore flank and bordered upward by the observed ground fractures [Gruppo di lavoro IREA-CNR & INGV, 2016]. Thus, ongoing studies are focusing on investigating the possible role of surface gravitational phenomena to the surface displacement observed along the Mt. Vettore flank.

Field observation reveal that, from a geological/geotechnical point of view, the SW flank of Mt. Vettore is covered in places by a thin layer (lower than 5 meters) of loose scree and talus deposits not exceeding few meters in

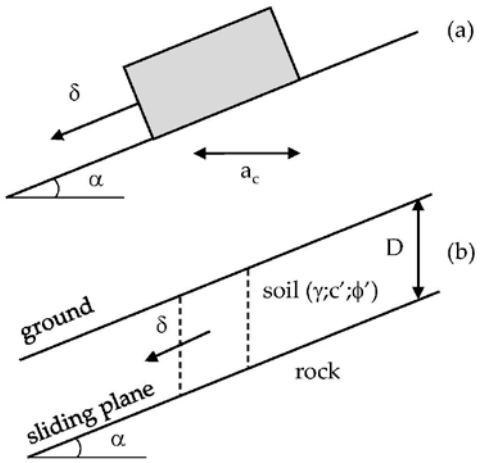

Figure 2: *Analogy between (a) block resting on inclined plane and (b) landslide on an infinite slope scheme.*

thickness and with variable grain size. [Pierantoni et al., 2013] (Figure 1b). Very often, the bedrock crops out along the slope, in the hanging wall of the ruptured Mt. Vettore and Vettoretto faults. In this work, we assess the stability of talus sediments during the M_W 6.0 earthquake shaking in order to identify the possible contribution of gravitational phenomena on the observed ground fractures.

II. Methods

Seismically-induced slope displacements of the sediment covering the Mt. Vettore flank were estimated following a permanent-displacement approach [Jibson, 2011] with the Newmark [1965] sliding-block method. In its simplest form, Newmark's method models a landslide as a rigid block that slides on an inclined plane (Figure 2a). The block has a known critical acceleration (a_c), i.e., the base acceleration that must be exceeded for a landslide block to begin moving relative to its base. A strong-motion record of interest is then selected, and those parts of the record exceeding the critical acceleration are integrated twice to obtain the velocity-time history and the cumulative displacement of the landslide block (δ).

The critical acceleration depends on the sliding mechanism and is determined by iteratively conducting pseudostatic limit-equilibrium analyses until a ground acceleration is found yielding a safety factor of 1 (i.e., the instability of the slope).

In particular, the expected movement of the debris is essentially translational instead of rotational [Varnes, 1978], given the low thickness of the debris with respect to its length and the bedrock immediately beneath. Thus, pseudostatic limit-equilibrium analyses are performed with reference to the infinite slope scheme, using the Bishop method and considering dry conditions (Figure 2b). For an infinite slope, the critical acceleration is given by equation 1.

$$a_c = \left(\frac{c'}{\gamma \cdot D \cdot \cos\alpha \cdot (1 + \tan\alpha \cdot \tan\phi')} + \frac{\tan\phi' - \tan\alpha}{1 + \tan\alpha \cdot \tan\phi'} \right) g \quad (1)$$

where g is the gravitational acceleration, γ is the unit weight of the soil, D is the thickness of the debris, α is the inclination of the sliding plane (corresponding to the slope angle), and ϕ' and c′ are the soil friction angle and cohesion.

The talus sediments are assumed cohesionless as they are constituted by clast-supported, loose or poorly cemented heterometric carbonate clasts, ranging from very angular to little or moderately rounded [Pierantoni et al., 2013]. Thus c′=0 in equation (1), hence the critical acceleration depends on the friction angle and slope inclination only.

Strong-motion records of the M_W 6.0 event have been used in the analysis. Horizontal acceleration time-histories from the nearest stations to the study area (RQT and NRC in Figure 1a) have been checked to select a proper acceleration record. In particular, the horizontal component from the RQT station (Figure 3a) has been selected as it presents a lower mean period (T_m) and higher Arias intensity (I_a) and significant duration (D_{5-95}) with respect to the NRC record (Table 1). The vertical components were neglected.

Table 1: *Selected ground motion records (http://esm.mi.ingv.it.)*

Name	Comp.	PGA	T_m	D_{5-95}	I_a
RQT.HGE	EW	0.45	0.16	6.9	1.53
NRC.HGE	EW	0.36	0.44	6.0	1.05

PGA = peak ground acceleration (g)
T_m = mean period (s)
D_{5-95} = significant duration (s)
I_a = Arias intensity (m/sec)

Laboratory model tests and analyses of earthquake-induced landslides in natural slopes confirm that Newmark's method can fairly accurately predict slope displacements if slope geometry, soil properties, and earthquake ground motions are known [Jibson, 2011]. However, given the uncertainties on the model parameters, the downslope displacements of the debris have been estimated through a parametric analysis (Table 2).

In particular, slope inclination varies between 28° and 34° according to the maximum and minimum inclinations of the Mt. Vettore flank (Figure 1d); friction angle varies between 32° and 40° according to literature data on similar material [Marsal, 1973; Albano et al., 2015]; and the peak acceleration of the RQT record

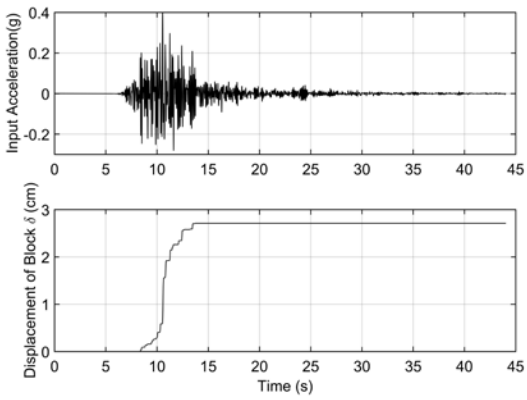

Figure 3: *Example application of the Newmark's method. The RQT strong-motion is scaled at 0.4g, the slope inclination is 30° and the soil friction angle is 36° (a_c =0.11g).*

is scaled between 0.2g and 0.5g, according to the PGA associated to the M_L 6.0 event. (http://shakemap.rm.ingv.it/).

Table 2: *Parameters and values adopted in the parametric analysis.*

Parameter		Range		Increment
name	symbol	min	max	
Slope angle (°)	α	28	34	2
Friction angle (°)	ϕ	32	40	2
PGA (g)	a_g	0.2	0.5	0.1

III. Results

The application of the Newmark's method provides the cumulated downslope displacements δ (parallel to the slope) for a given strong-motion record (Figure 3b). The maximum downslope displacements obtained for each combination of the parameters listed in Table 2 are displayed in Figure 4 against slope angle, friction angle and PGA. The expected downslope displacements are on the order of

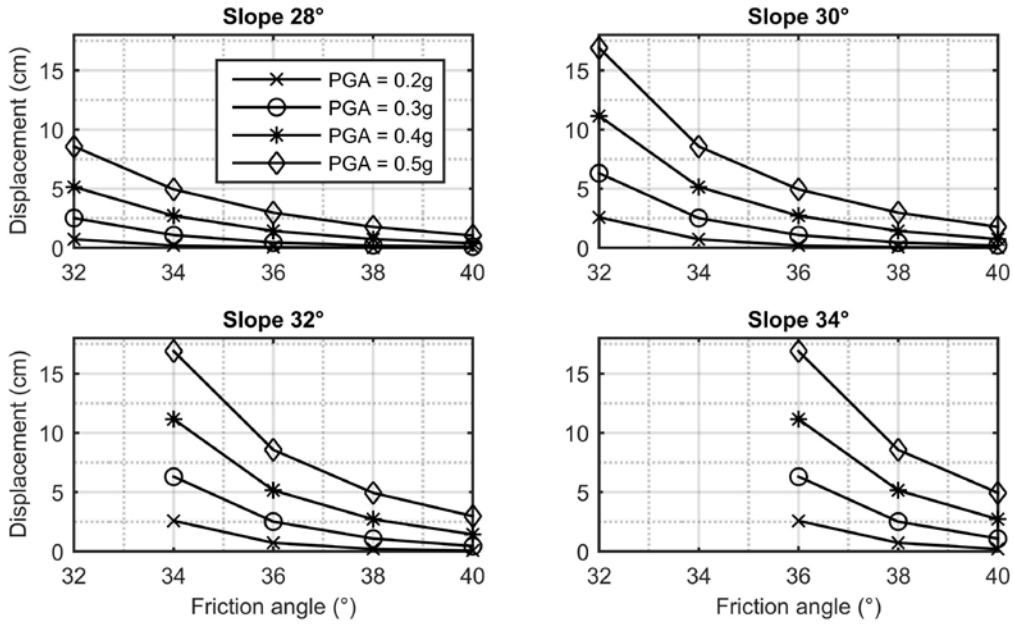

Figure 4: *Results of the parametric analysis expressed as the maximum downslope displacements versus slope angle, friction angle and PGA.*

some tens of centimeters. In particular, downslope displacements decrease with increasing friction angle and increase with increasing PGA and slope inclination. The slope is stable for low PGA (0.2g) and high friction angles (38° – 40°) only.

According to the geomorphological and geotechnical features of the study area, we assumed as representative conditions a slope angle of 30°- 32°, a friction angle of 36° - 38° and a PGA between 0.4g and 0.5g. Under these assumptions, the modelled downslope displacements are between 2 – 10 cm.

IV. Discussion and conclusions

The performed parametric analyses indicate that probably talus sediments have slipped seismically during the M_W 6.0 event. However, the significance of the modeled displacements and their possible effect on the ground must be judged according to the assumed modelling hypotheses.

A key assumption of Newmark's method is that it treats a landslide as a rigid-plastic body, i.e., the mass does not deform internally and experiences no permanent displacement at accelerations below the critical level. In spite of this strong simplification, the method provides good results for thinner and relatively stiff landslides [Jibson, 2011] as in the studied case, then the predicted displacements are reliable.

Neglecting the vertical component of the seismic input does not dramatically change the results because the vertical component is less relevant in slope stability analysis. Moreover, seismically induced ground compaction is not expected on coarse, well-sorted and clast-supported granular materials.

Finally, the aftershock contribution to the sliding of the debris is negligible because the measured PGAs in the study area are much

lower than 0.2g (http://shakemap.rm.ingv.it/). Only the M_W 5.4 event reached a PGA of 0.22g in the study area, thus producing a displacement of about 1 cm (Figure 4).

Shallow landslides commonly are triggered at much lower displacement levels respect to deep landslides, therefore displacements of 2-10 cm are sufficient to lead macroscopic ground cracking and failure in most soils [Jibson, 2011]. However, the observed fractures show a vertical offset up to 30 cm and a horizontal component (opening) up to 20 cm has been also observed in several sectors [EMERGEO Working Group, 2016]. Thus, the hypothetical plane of the landslide could be at least 45° steep.

The modelled displacements cannot explain the field evidence both in magnitude and slope inclination. Moreover, it should be considered that the presence of a continuous cover of slope debris is actually contradicted by the field surveys. Indeed, at many places where ground cracks have been observed, the carbonate bedrock has been detected both in the footwall and in the hangingwall.

In the whole, gathered data suggest that the fractures along the Mt. Vettore flank are the combination of primary faulting related to tectonics and gravitational phenomena. At this time, it is not possible to quantify the different contributions. Further studies currently in progress are need to assess the relative contribution of tectonic and gravitational phenomena on the observed vertical and horizontal throws.

References

Albano, M., G. Modoni, P. Croce, and G. Russo (2015), Assessment of the seismic performance of a bituminous faced rockfill dam, Soil Dyn. Earthq. Eng., 75, 183–198, doi:10.1016/j.soildyn.2015.04.005.

EMERGEO Working Group (2016), The 24 August 2016 Amatrice Earthquake: Coseismic Effects.

Gruppo di Lavoro INGV sul terremoto di Amatrice (2016), Secondo rapporto di sintesi sul Terremoto di Amatrice Ml 6.0 del 24 Agosto 2016 (Italia Centrale).

Gruppo di lavoro IREA-CNR & INGV (2016), Sequenza sismica di Amatrice: aggiornamento delle analisi interferometriche satellitari e modelli di sorgente.

ISIDe Working Group (2016), Italian Seismological Instrumental and Parametric Data-base (ISIDe), , doi:10.13127/ISIDe.

Jibson, R. W. (2011), Methods for assessing the stability of slopes during earthquakes-A retrospective, Eng. Geol., 122(1–2), 43–50, doi:10.1016/j.enggeo.2010.09.017.

Marsal, R. J. (1973), Mechanical properties of rockfill, in Embankment Dam Engineering, vol. Casagrande, pp. 109–200, John Wiley and Sons, New York.

Newmark, N. M. (1965), Effects of earthquakes on dams and embankments, Geotechnique, 15, 139–159.

Pierantoni, P., G. Deiana, and S. Galdenzi (2013), Stratigraphic and structural features of the Sibillini Mountains (Umbria-Marche Apennines, Italy), Ital. J. Geosci., 132(3), 497–520, doi:10.3301/IJG.2013.08.

Varnes, D. J. (1978), Slope Movement Types and Processes, Transp. Res. Board Spec. Rep., (176), 11–33, doi:In Special report 176: Landslides: Analysis and Control, Transportation Research Board, Washington, D.C.